30TH INTERNATIONAL COSMIC RAY CONFERENCE

ICRC 2007 Proceedings - Pre-Conference Edition

Electron Injection at Quasi-Perpendicular Supernova Remnant Shocks

T. AMANO[1], M. HOSHINO[1]
[1] *Department of Earth and Planetary Science, University of Tokyo*
amano@eps.s.u-tokyo.ac.jp

Abstract: Electron injection process at high Mach number collisionless quasi-perpendicular shock waves is investigated by means of one-dimensional electromagnetic particle-in-cell simulations. We find that energetic electrons are generated through the following two steps: (1) electrons are accelerated nearly perpendicular to the local magnetic field by shock surfing acceleration at the leading edge of the shock transition region. (2) the preaccelerated electrons are further accelerated by shock drift acceleration. As a result, energetic electrons are preferentially reflected back to the upstream. Shock surfing acceleration provides sufficient energy required for the reflection. Therefore, it is important not only for the energization process by itself, but also for triggering the secondary acceleration process. We also present a theoretical model of the two-step acceleration mechanism based on the simulation results, which can predict the injection efficiency for subsequent diffusive shock acceleration process. We show that the injection efficiency obtained by the present model agrees well with the value obtained by Chandra X-ray observations of SN 1006. At typical supernova remnant shocks, energetic electrons injected by the present mechanism can self-generate upstream Alfven waves, which scatter the energetic electrons themselves.

Introduction

It is widely believed that cosmic rays (CRs) with energies up to about $10^{15.5}$ eV are produced at supernova remnant (SNR) shocks. Koyama et al. (1995) indeed showed the direct evidence of cosmic-ray electrons accelerated to energies about 10 TeV. Diffusive shock acceleration (DSA; e.g., Blandford & Eichler, 1987) is the most plausible shock acceleration theory, which has been applied to many problems including in-situ observations of shocks in the heliosphere. One of the most crucial issues in DSA theory is the injection problem: there must be some other acceleration mechanism to provide a seed population for this process.

An early theoretical effort to explain the strong energization of electrons at SNR shocks has done by Papadopoulos (1988). He showed that the Buneman instability can be excited in the shock transition region of perpendicular shocks with Mach number typical of SNR shocks due to the presence of the so-called reflected ions. The instability gives rise to very rapid electron heating, which triggers the secondary ion acoustic instability and further electron heating. This two-step energization mechanism of electrons was later discussed by Shimada & Hoshino (2000) using a particle-in-cell (PIC) simulation code in which both ions and electrons are treated as macroparticles. They found strong electron heating and acceleration in the shock transition region via electron shock surfing/surfatron acceleration (SSA; e.g., Hoshino, 2001; McClements et al., 2001). Since the SSA may provide a clue to the electron injection problem, it has attracted considerable attention and been investigated in detail (e.g., Hoshino & Shimada, 2002; Schmitz et al., 2002). However, previous studies of SSA are restricted to the case of strictly perpendicular shocks. Here, we present numerical simulation results of very high Mach number quasi-perpendicular shocks relevant to SNR shocks. It is shown that energetic electrons are produced by SSA in quasi-perpendicular shocks as well as strictly perpendicular shocks. The energetic electrons generated by SSA are further accelerated by the so-called fast Fermi process or shock drift acceleration (SDA; Wu, 1984; Leroy & Mangeney, 1984). Since the SDA can be considered to be the mirror reflection process in the de Hoffmann-Teller frame, the momentum of particles reflected by this process is increased by $\Delta p = 2mV_0/\cos\theta_{\rm Bn}$, where m, V_0, and $\theta_{\rm Bn}$ are the particle mass, the shock speed, and the shock angle, respectively. This two-step acceleration mechanism is important for providing a seed population for subsequent DSA process. The energies of reflected electrons are indeed large enough to be accelerated by the DSA process.

Simulation Results

A one-dimensional electromagnetic PIC code, in which both ions and electrons are treated as macroparticles, is used to investigate the electron energization process in a self-consistent shock structure. The shock waves are produced by the so-called injection method: A high-speed plasma consisting of electrons and ions is injected from the left-hand boundary of a one-dimensional simulation system and travels toward positive x. The plasma carries a uniform magnetic field ($B_{\rm x}$, $B_{\rm z}$). The right-hand boundary is the reflecting wall, where all particles and waves are reflected. A shock wave is formed through the interaction between the incoming and the reflected plasma and propagates in the negative x-direction. The simulation is performed in the downstream rest frame. We used 100 particles for each species in each computational cell. The grid size is comparable to the Debye length, and the simulation box consists of 51,200 grids. The plasma parameters are as follows: a ratio of ion to electron mass $m_{\rm i}/m_{\rm e} = 100$, the plasma to the electron cyclotron frequency $\omega_{\rm pe}/\Omega_{\rm ce} = 20$, upstream plasma beta $\beta_{\rm e} = \beta_{\rm i} = 0.08$ ($\beta_{\rm j} \equiv 8\pi n T_{\rm j}/B^2$), where n, $T_{\rm j}$, and B are the density, temperature, and magnetic field strength, respectively. The upstream Alfvén speed becomes $5 \times 10^{-3}c$, where c is the speed of light. We use a plasma injection 4-velocity of $U_0 = 5 \times 10^{-2}c$. The Alfvén Mach number of the resultant shock wave is $M_{\rm A} \simeq 15$ in the shock rest frame. In the following, the magnetic and electric field will be given in units of the z-component of the upstream magnetic field $B_{0,\rm z} = B_0 \sin\theta_{\rm Bn}$ and the motional electric field $E_{0,\rm y} = V_0 B_{0,\rm z}/c$, respectively. The length, density, velocity and energy are normalized to the electron inertial length $c/\omega_{\rm pe}$, the density, the bulk velocity and the bulk energy in the upstream, respectively.

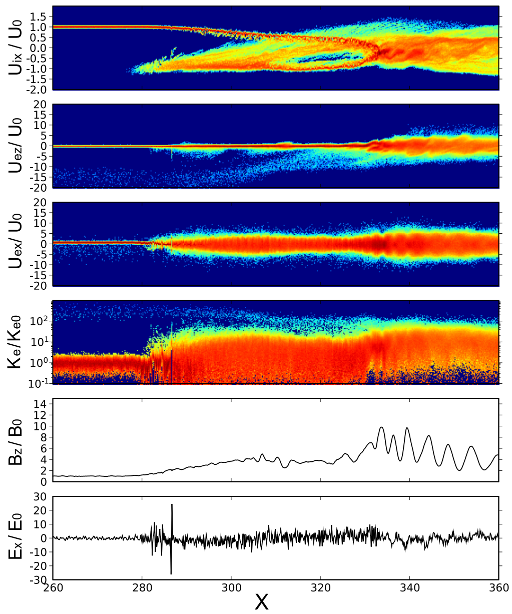

Figure 1: From top to bottom: ion phase-space diagram in $(X, U_{\rm ix})$, electron phase-space diagrams in $(X, U_{\rm ez})$, $(X, U_{\rm ex})$, and $(X, K_{\rm e})$, the magnetic field $B_{\rm z}$, and the electric field $E_{\rm x}$. Colors in the phase-space diagrams represent the logarithm of the particle count in each bin.

First, we present simulation results of a shock with $\theta_{\rm Bn} = 80°$. Figure 1 shows the overall structure of the shock transition region at $\omega_{\rm pe}t = 12,000$. The basic structure of the shock transition region is similar to those obtained in previous simulation studies of strictly perpendicular shocks (e.g. Hoshino & Shimada, 2002). We can see strong electrostatic waves excited by the Buneman instability in the leading edge of the shock transition region, which involves strong energization of the upstream electrons. The heating and acceleration of electrons due to the turbulence occur on a very short time scale. If we look deeper inside the shock transition region, the preheated electrons trigger the ion acoustic instability, and the associated heating of incoming ions is evident in the top panel.

In addition to these features, which are common to strictly perpendicular shocks, we clearly find energetic electrons streaming away from the shock

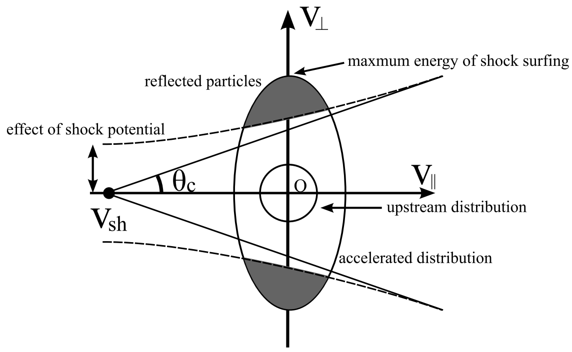

Figure 2: Schematic illustration of surfing and drift acceleration. The shaded region represents the reflected particles.

front along the magnetic field. These parallel escaping energetic electrons can be seen in the second panel, which represents the z-component of the electron 4-velocity. Note that this velocity component is almost parallel to the magnetic field. Detailed investigation by Amano & Hoshino (2007) has shown that these reflected electron are produced via SSA followed by SDA, — that is, the reflected electrons suffer rapid energization by SSA when they enter the shock transition region and are reflected by the mirror force. Although SDA process is extremely efficient at nearly perpendicular high Mach number shocks, the well-known difficulty is that the number of upstream particles outside the loss cone is quite small in such shocks. It can be readily shown that the upstream thermal electrons cannot be reflected by the shock in the present simulation parameters. However, our simulation results demonstrate that the reflection does indeed take place because of plasma microinstabilities in the shock transition region: The cold upstream electrons are energized by SSA at the leading edge of the shock transition region, so that a non-negligible fraction of electrons escape the loss cone. These preaccelerated electrons are subjected to SDA and reflected back upstream. A schematic illustration of the reflection initiated by SSA is shown in Figure 2. In this acceleration mechanism, SSA plays a crucial role in triggering the secondary acceleration. The important point is that SSA produces power-law like energy spectra in the shock transition region (see Amano & Hoshino, 2007).

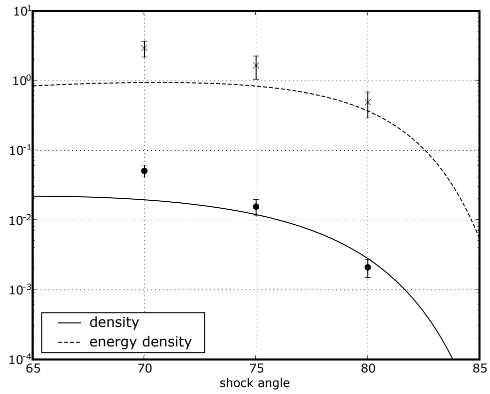

Figure 3: The density (filled circles) and the energy density (crosses) of the reflected electrons measured in the upstream. The solid and dashed lines represents the model calculation.

Electron Injection at SNR Shocks

Since the reflected electrons can self-generate upstream Alfvén waves at shocks with Mach number typical of SNR shocks, we can recognize the reflection of energetic electrons as “injection” into a subsequent DSA process. Then, we consider a ratio of the reflected electron to the upstream density to be the injection efficiency. Based on the simulation results, we constructed a theoretical model of the two-step acceleration mechanism that can predict the injection efficiency as a function of shock angle (see, for detail Amano & Hoshino, 2007).

Figure 3 shows a comparison of the injection efficiency between the simulation results and the model with an artificial mass ratio of $m_{\rm i}/m_{\rm e} = 100$. One can see a good agreement between the model and the simulation results. By utilizing this model, we estimated the injection efficiency of SNR shocks. We found that the peak injection efficiency reaches $\sim 10^{-4}$ at $\theta_{\rm Bn} \sim 80°$, which is comparable to values obtained from SN 1006 observations (e.g., Bamba et al., 2003).

Discussion and Conclusions

We have studied a rapid energization of electrons at very high Mach number, quasi-perpendicular shocks using one-dimensional electromagnetic particle-in-cell code. It is found that highly energetic electrons are generated through two successive acceleration processes; i.e., SSA followed by SDA produces reflected, energetic electrons. The reflected electrons can be a seed population for subsequent DSA process. It is also shown that the present mechanism can explain the injection efficiencies obtained from SN 1006 observations. The most efficient electron injection takes place at shocks with $\theta_{\rm Bn} \sim 80^\circ$. This is consistent with the observational constraint that the shock angle should be sufficiently large ($\theta_{\rm Bn} \gtrsim 80$) in order to explain observed thickness of extremely thin nonthermal filaments with a typical interstellar magnetic field of a few μG (Bamba et al., 2003). However, there are indications of highly amplified magnetic field at some SNR shocks (Bamba et al., 2005), which may be explained by nonlinear magnetic field amplification scenario (Bell, 2004). Although this scenario relaxes the constraint on the shock angle, we think quasi-perpendicular shocks still favor the efficient electron injection. Furthermore, subsequent energy gain through DSA process in quasi-perpendicular shocks is also much more efficient than in quasi-parallel shocks (Jokipii, 1987).

Concerning the turbulence in the upstream region of quasi-perpendicular shocks, the amplitude of self-generated Alfvén waves may be estimated by assuming the all electron beam energy is converted to wave energy;

$$\left(\frac{\delta B}{B_0}\right)^2 \sim \frac{n_{\rm b} m_{\rm i} V_0^2}{B_0^2/4\pi} = \frac{n_{\rm b}}{n_0}\frac{m_{\rm e}}{m_{\rm i}}\left(\frac{M_{\rm A}}{\cos\theta_{\rm Bn}}\right)^2,$$

where $n_{\rm b}/n_0$ is the electron injection efficiency. For very young SNR shocks with $M_{\rm A} \sim 1000$ and $n_{\rm b}/n_0 \sim 10^{-4}$, $\theta_{\rm Bn} \sim 80^\circ$, this leads to $(\delta B/B_0)^2 \gtrsim 1$. Since shocks in such a highly turbulence medium may enhance the proton injection (Giacalone, 2005), understandings of nonlinear interaction between energetic particles and upstream plasma is quite important as well as the injection process itself.

In the present study, we have used one-dimensional PIC code in which plasma instabilities propagating transverse to the shock normal (e.g., lower-hybrid-drift instability) are neglected. We note that it is important to investigate a further energization through these instabilities which may result in the increase of the injection efficiency.

Acknowledgements

This work was supported by ISAS/JAXA and the Solar-Terrestrial Environment Laboratory, Nagoya University. T. A. is supported by a JSPS Research Fellowship for Young Scientists.

References

Amano, T., & Hoshino, M., Astrophys. J., 661, 190. 2007

Bamba, A., Yamazaki, R., & Hiraga, J. S., Astrophys. J., 632, 294. 2005

Bamba, A., Yamazaki, R., Ueno, M., & Koyama, K., Astrophys. J., 589, 827. 2003

Bell, A. R., Mon. Not. R. Astron. Soc., 353, 550. 2004

Blandford, R., & Eichler, D., Phys. Rep., 154, 1. 1987

Giacalone, J., Astrophys. J. Lett., 628, L37. 2005

Hoshino, M., Prog. Theor. Phys. Suppl., 143, 149. 2001

Hoshino, M., & Shimada, N., Astrophys. J., 572, 880. 2002

Jokipii, J. R., Astrophys. J., 313, 842. 1987

Koyama, K., Petre, R., Gotthelf, E. V., Hwang, U., Matsuura, M., Ozaki, M., & Holt, S. S., Nature, 378, 255. 1995

Leroy, M. M., & Mangeney, A., Ann. Geophys., 2, 449. 1984

McClements, K. G., Dieckmann, M. E., Ynnerman, A., Chapman, S. C., & Dendy, R. O., Phys. Rev. Lett., 87, 255002. 2001

Papadopoulos, K., Astrophys. Space Sci., 144, 535. 1988

Schmitz, H., Chapman, S. C., & Dendy, R. O., Astrophys. J., 579, 327. 2002

Shimada, N., & Hoshino, M., Astrophys. J. Lett., 543, L67. 2000

Wu, C. S., J. Geophys. Res., 89, 8857. 1984